Short range order transformation and magnetostriction of $Fe_{83}Ga_{17}$ ribbons*

Zhu Jie(朱 洁)[a)†], Peng Fu-Ling(彭福玲)[a)], Fang Mei-Ling(方美玲)[a)], Li Ji-Heng(李纪恒)[a)], Gao Xue-Xu(高学绪)[a)], and Yu Rong-Hai(于荣海)[b)]

[a)] *State Key Laboratory for Advanced Metals and Materials, University of Science and Technology Beijing, Beijing* 100083, *China*
[b)] *School of Materials Science and Engineering, Beihang University, Beijing* 100191, *China*

(Received 29 November 2010; revised manuscript received 23 December 2010)

The relationship between magnetostriction and structure of melt-spun $Fe_{83}Ga_{17}$ ribbons are investigated by XRD and Mössbauer spectrum technique (MS). As the heat-treatment temperature increases from 650°C to 800°C, the magnetostriction coefficient of $Fe_{83}Ga_{17}$ ribbon first increases and then decreases. The largest magnetostriction coefficient (−578.4 ppm) is achieved in those specimens quenched at 750°C. According to the XRD and Mössbauer spectrum analysis, a small quantity of DO_3 phase is precipitated in $Fe_{83}Ga_{17}$ ribbons when quenched from 650°C and the DO_3 phase is gradually transformed into B2-like phase if quenched at higher temperature. However, both DO_3 and B2-like phases disappear when the temperature increases up to 800°C. From this point of view, B2-like phase might be beneficial to the enhancement of magnetostrictive properties of melt-spun ribbons.

Keywords: Fe–Ga alloy, magnetostriction, Mössbauer spectroscopy, short range order

PACS: 75.80.+q, 33.45.+x, 64.60.Cn **DOI:** 10.1088/1674-1056/20/5/057504

1. Introduction

The Fe–Ga alloy has aroused the much interest due to its good mechanical property, large magnetostriction, low cost and outstanding resistance to harsh environments.[1] Recent research has found that the magnetostriction of melt-spun Fe–Ga ribbon was about 130 ppm (1 ppm = 10^{-6}), which was much larger than that of the directionally solidified Fe–Ga rod.[2] It was reported that the magnetostriction of quenched $Fe_{85}Ga_{15}$ ribbons was −1300 ppm.[3] Generally speaking, large magnetostriction of Fe–Ga alloys was attributed to the orderly arranged Ga atoms. Particularly, the modified DO_3 structure (also referred as B2-like) was considered as a major factor for this phenomenon, where Ga atoms were arranged in pairs, instead of 4 or 8 atoms neighbouring to Fe atom.[4] In addition, theoretical calculation showed that the magnetic anisotropy of modified DO_3 structure was stronger than those of A2, B2 and DO_3 structure.[5] The experiment found that the light diffraction peaks of DO_3 only appeared in certain conditions.[6] For example, Liu *et al.* observed diffraction pattern of DO_3 through the electron microscope analysis.[7] However, it is difficult to determine whether there exist Ga–Ga pairs in the modified DO_3 structure by traditional analytical tools since their structures are similar to the DO_3 structure.

Mössbauer spectrum, which is available for bringing out information about atoms neighbouring Fe atoms, is the best experimental tool for short-range order study. Previous reports on Mössbauer studies are a great help in understanding the structures of Fe–Ga alloys. Newkirk and Tsuei[8] confirmed that ordered DO_3 structure appeared in an equilibrium state of $Fe_{80}Ga_{20}$ alloys after long-term annealing; Perduta *et al.*[9] found the ordered DO_3 structure in ball milling $Fe_{80}Ga_{20}$ alloy sample; Gaudet *et al.*[10] studied Mössbauer spectra of Fe–Ga alloys prepared by mechanical alloying; Borrego *et al.*[11] investigated the effect of Ga content on the magnetic hyperfine field (HF) through Mössbauer spectrometry; Basumatary *et al.*[12] presented the evolution of short-range order in Fe–Ga alloys using a continuous spectrum fitting method. Dunlap *et al.*[13,14] pointed out that the nonmagnetic elements Ga and Al tend to form cluster in Fe–Ga and Fe–Ga–Al thin films.

Much attention has been focused on the magnetic HF and the centre shifts of various sub-spectra. How-

*Project supported by the National Basic Research Program of China (Grant No. 2010CB934602).
†Corresponding author. E-mail: jiezhu@ustb.edu.cn
© 2011 Chinese Physical Society and IOP Publishing Ltd

ever, according to the author's knowledge, there have been few reports on the quadrupole splittings (QSs) of sub-spectra. QS is the interaction between the nucleus moment and the local electric field gradient (EFG). Thus, the positive or negative value of QS could characterize the Mössbauer nucleus shape and indirectly give out the EFG around Mössbauer nucleus, *i.e.*, around the Fe atom in the case of Fe–Ga alloy. If the different values of QS are caused by occupancy of coordination atoms and the possible occupancies of atoms around the Fe atom are clear, then we can qualitatively analyse the atom occupancy through the value of QS. In particular, for the sub-spectrum of four Ga atoms neighbouring to Fe atom, the EFG around the Fe atom will be zero if its QS parameters are zero. Otherwise, it does not equal zero. Therefore, the QS could be very useful for determining whether there exist Ga–Ga pairs in Fe–Ga alloys or not.

In this study, the melt-spun $Fe_{83}Ga_{17}$ ribbons are heat-treated at different temperatures. The phase structure and evolution of short range order are analysed by XRD and Mössbauer spectrum.

2. Experiment

The cast rods each with 10 mm in diameter were prepared from Fe (99.99% pure) and Ga (99.9% pure) in a vacuum melting furnace. The $Fe_{83}Ga_{17}$ ribbons were produced by melt-spinning equipment in an argon atmosphere with a wheel speed of 12 m/s. Then they were annealed at 650, 700, 750°C for 3 h in evacuated quartz tubes and water-quenched sequentially. The quenched ribbons each are about 70 μm in thickness.

Magnetostriction was performed on JDAW-2011 magnetostriction measurement equipment. The X-ray diffraction spectrum was taken by D / MAX-RB X-ray diffractometer with Cu $K\alpha$ (λ = 1.5406 Å, 1 Å = 0.1 nm) radiation.

The Mössbauer spectra of $Fe_{83}Ga_{17}$ ribbons were measured by MS-500 type Mössbauer spectrometer at room temperature. In order to ensure an adequate statistical error, the accumulative count of each spectrum was greater than 10^6. The Mössbauer spectrum data were analysed by the MOSFE program and the parameters were calculated with pure α-Fe calibration. Each sub-spectrum on Fe nucleus was composed of six Gaussian lines and least squares method was employed for the HF lines fitting process.

3. Results

3.1. Magnetostriction

The addition of the non-magnetic element Ga to bcc Fe greatly increases the magnetostriction coefficient λ of Fe by a few times, or even 100 times. Previous studies showed that magnetostriction coefficient of Fe–Ga ribbon was negative. Figure 1 exhibits the magnetostriction curves of the melt-spun $Fe_{83}Ga_{17}$ ribbons before and after heat treatment. It can be seen that the λ values of all samples gradually increase as the external magnetic field rises. The magnetostrictive properties of $Fe_{83}Ga_{17}$ alloys have been improved by different degrees after heat treatment. Particularly, compared with the magnetostriction value of −459.6 ppm of melt-spun ribbons, the magnetostriction reaches a maximum value of −578.4 ppm after the ribbons have been heat-treated at 750°C. In addition, the magnetostriction becomes saturated under a magnetic field of 700 kA/m except for the ribbons which are heat-treated at 650°C and the as-spun ribbons. So, in our experiments, the best heat treatment for melt-spun $Fe_{83}Ga_{17}$ ribbons is at 750°C for 3 h and low field magnetostrictive properties are also greatly enhanced.

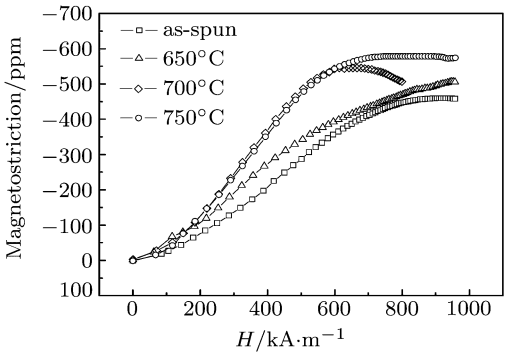


Fig. 1. Magnetostriction curves of $Fe_{83}Ga_{17}$ ribbons quenched at different temperatures.

3.2. X-ray diffraction results

Figure 2 shows the XRD spectra of melt-spun $Fe_{83}Ga_{17}$ ribbons before and after heat treatment. No evident super-lattice peaks are found in the spectra, in particular around 26.5° and 55°, which is indicative of long range order of DO_3 phase. Three strong diffraction peaks, i.e., (110), (200) and (211), suggest that the basic structure of these ribbons be the disordered A2 structure, though there were some differences in peak shape and position.

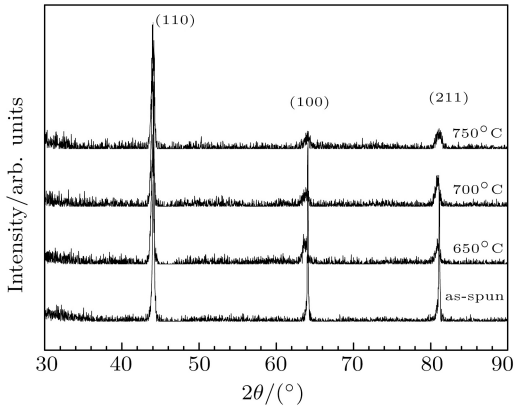


Fig. 2. XRD diffraction spectra of $Fe_{83}Ga_{17}$ ribbons heat-treated at different temperatures.

Figure 3 demonstrates that annealing and subsequent quenching cause a slight position shift and shape change of (110) diffraction peak as a result of evolution of short-range order. The major peak of as-spun ribbon appears at 44.17° while the major peak of heat-treated ribbons occurs at 43.96°. It can be interpreted as two kinds of short-range orders taking place in heat-treated ribbons or phase separation in Fe–Ga alloys with different Ga content.

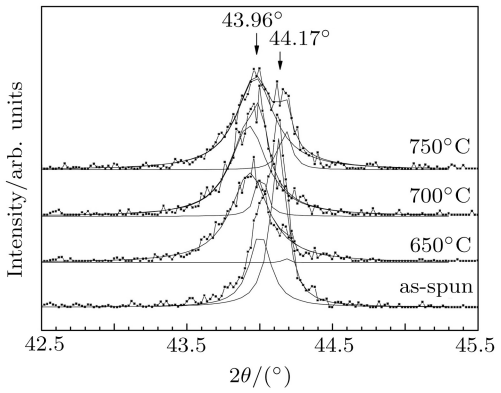


Fig. 3. Partially enlarged (110) peaks of $Fe_{83}Ga_{17}$ ribbons heat-treated at different temperatures.

The crystal lattice parameters of the two peaks are 2.910 and 2.898 nm, which were larger than those of $Fe_{83}Ga_{17}$ containing A2 or DO_3 structure.[12] From the neutron diffraction results,[15] it follows that the lattice parameter of Fe–Ga ribbon calculated from the low angle (110) peak is greater than those from all other peaks. This is the same as our case.

Splitting of XRD peak has been observed in Fe–Ga alloy by previous researchers. For example, splitting of (200) diffraction peak appeared in thin $Fe_{85}Ga_{15}$ ribbon.[3] Lograsso and Summers[16] pointed out that the (200) diffraction peak was composed of peaks at 63.709° and 64.145° and also gave the fitting results of (211) peak split. All other literature did not report on the (110) peak splitting. The (110) diffraction peak was fitted to two sub-peaks as shown in Fig. 3. The diffraction angle and the relative area of peak are listed in Table 1.

Table 1. Fitting result for $Fe_{83}Ga_{17}$ as-spun ribbon (110) peak.

Heat treatment	$2\theta_1/(°)$	$2\theta_2/(°)$	Relative area	
			$(2\theta_1)$	$(2\theta_2)$
as-spun	44.00	44.13	0.371	0.629
650 °C	43.98	44.18	0.989	0.011
700 °C	43.93	44.20	0.973	0.027
750 °C	43.97	44.17	0.837	0.163

For the as-spun ribbon, the major peak is at 44.17° and the left shoulder refers to the contribution of the 40.00° peak. As can be seen from Table 1, with the increase in heat treatment temperature, the (110) diffraction peak gradually split into two diffraction peaks θ_1 and θ_2 and the relative peak area of θ_2 increases also.

Therefore, it may be speculated that a short-range disorder appears after heat treatment. Peaks θ_1 and θ_2 represent two kinds of arrangements of Ga atoms in Fe–Ga. One is that the Ga atoms arrange randomly, similar to disordered occupation as A2 phase. The other is that the Ga atoms distribute with a certain order, which could be described as DO_3 phase or B2-like phase. Thus, Mössbauer spectrum is required to confirm the existence of B2–like phase.

3.3. Mössbauer spectra results

In the bcc crystal structure, each Fe atom core is surrounded by eight neighbours. Assuming that magnetic HF of Fe is influenced only by neighbouring atoms, the effect of next-neighbour atoms on Fe nucleus can be ignored. In this paper, $y$nn means that there are y Fe atoms surrounding the Fe nucleus. Accordingly, there are $(8-y)$ Ga atoms neighbouring the Fe nucleus.

According to Blachouski's calculation model and the continuous spectrum-decomposition results,[17]

the initial values of the hyperfine field of 8nn, 7nn, 6nn, 5nn and 4nn are 34.71, 32.43, 29.63, 26.09 and 21.82 T, respectively. To fit spectrum, first, using fix peak intensity ratio I_3: I_2: I_1 to give a sub-spectrum and set the initial value hyperfine field of $y$nn. Secondly, open the central isomer shift (IS) and the quadrupole splitting parameters for free fitting and calculate them by employing the Gaussian method. Finally, obtain the best fitting results by adjusting the hyperfine interaction parameters. The experimental data and fitted sub-spectra are listed in Table 2 and displayed in Fig. 4.

Table 2. Fitting parameters of HF, IS, QS, the half width of the sub spectrum (HWHM) and the relative content Fe of each sub-spectrum versus heat treatment temperature.

Heat treatment	Sub-spectrum	HF /T	IS /mm·s^{-1}	QS /mm·s^{-1}	HWHM /mm·s^{-1}	Area ratio /%
as-spun	8nn	33.33 ± 0.07	0.08 ± 0.00	0.01 ± 0.01	0.24 ± 0.00	29.2
	7nn	31.11 ± 0.04	0.12 ± 0.00	-0.01 ± 0.01	0.20 ± 0.01	28.8
	6nn	29.07 ± 0.04	0.15 ± 0.01	-0.02 ± 0.01	0.20 ± 0.00	25.8
	5nn	26.69 ± 0.10	0.19 ± 0.01	-0.01 ± 0.01	0.17 ± 0.02	13.4
	4nn	24.25 ± 0.30	0.32 ± 0.04	-0.21 ± 0.09	0.13 ± 0.01	2.8
650 °C	8nn	33.76 ± 0.06	0.10 ± 0.00	0.00 ± 0.01	0.19 ± 0.01	20.8
	7nn	31.69 ± 0.04	0.12 ± 0.00	0.01 ± 0.01	0.18 ± 0.00	26.3
	6nn	29.78 ± 0.05	0.14 ± 0.01	-0.01 ± 0.01	0.20 ± 0.02	28.6
	5nn	27.24 ± 0.09	0.19 ± 0.01	-0.03 ± 0.02	0.23 ± 0.01	19.1
	4nn	23.28 ± 0.30	0.43 ± 0.02	-0.02 ± 0.05	0.22 ± 0.03	5.1
700 °C	8nn	33.57 ± 0.04	0.11 ± 0.00	0.01 ± 0.01	0.20 ± 0.01	21.9
	7nn	31.59 ± 0.03	0.11 ± 0.00	-0.02 ± 0.01	0.18 ± 0.01	28.6
	6nn	29.55 ± 0.03	0.15 ± 0.01	-0.02 ± 0.01	0.19 ± 0.02	27.3
	5nn	27.34 ± 0.06	0.19 ± 0.01	-0.03 ± 0.01	0.20 ± 0.01	18.7
	4nn	23.58 ± 0.20	0.40 ± 0.02	-0.33 ± 0.07	0.18 ± 0.03	3.5
750 °C	8nn	33.53 ± 0.05	0.09 ± 0.01	0.01 ± 0.01	0.20 ± 0.00	23.5
	7nn	31.57 ± 0.03	0.11 ± 0.01	-0.01 ± 0.01	0.17 ± 0.01	28.7
	6nn	29.63 ± 0.04	0.13 ± 0.01	-0.02 ± 0.01	0.19 ± 0.00	28.1
	5nn	27.43 ± 0.08	0.19 ± 0.01	-0.02 ± 0.02	0.21 ± 0.01	17.5
	4nn	23.61 ± 0.20	0.49 ± 0.02	-0.27 ± 0.07	0.11 ± 0.01	2.2

Figure 5 shows the evolution of fitting parameters after heat treatment. It can be seen from Fig. 5(a) that for the as-spun ribbons, the HF of 8nn to 5nn sub-spectrum is slightly smaller than that of heat-treated sample. The situation is opposite for 4nn sub-spectrum. Additionally, there is almost no change in HF of each sub-spectrum in heat-treated ribbon. In Fig. 5(b), as the heat treatment temperature rises, the relative content of Fe increases for the 6nn sub-spectrum but decreases for the other sub-spectra.

In Fig. 5(c), the value of IS increases with decreasing y value, which is the same as the result in Ref. [9]. Moreover, there is a significant difference in 4nn sub-spectrum between the as-spun and heat-treated ribbons, which indicates that their short-range orders are different from each other. This phenomenon is consistent with the XRD results depicted in Fig. 3.

In Fig. 5(d), the maximum QS values of sub-spectra are all close to zero. However, the QS values of 4nn sub-spectrum are negative except for those of the ribbons heat-treated at 650°C. A possible explanation for this is that the occupancy of four Ga atoms surrounding Fe nucleus has changed at the present heat treatment.

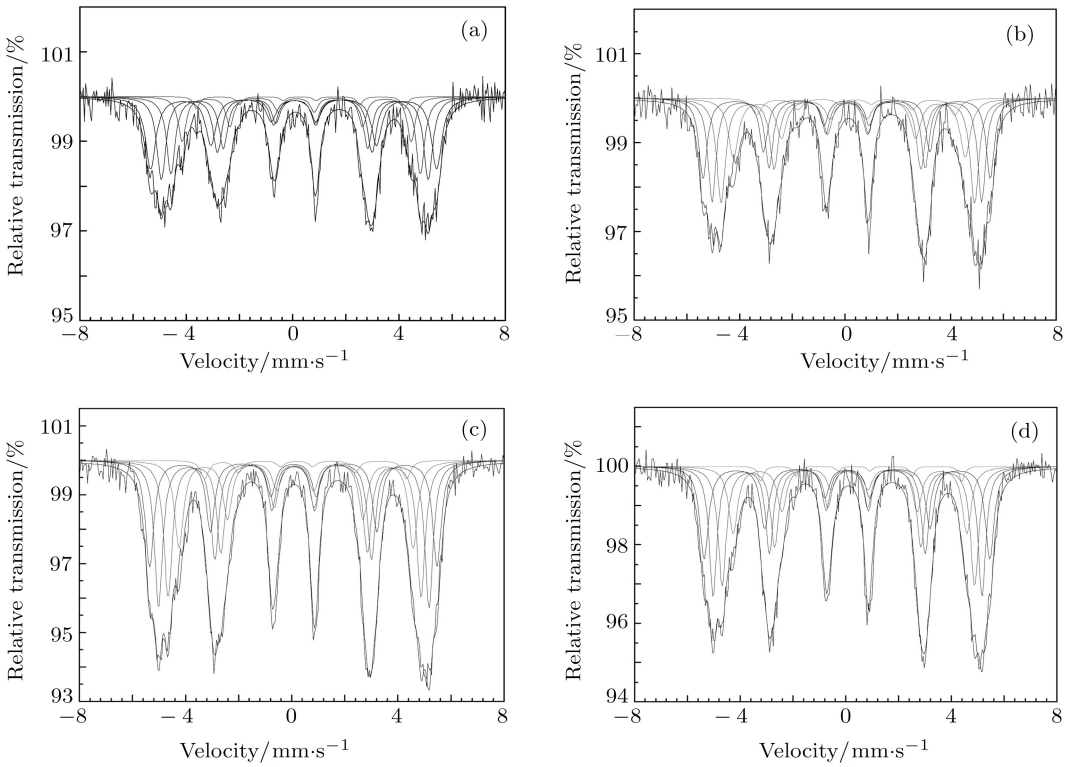


Fig. 4. Mössbauer spectra and fitting results of melt-spun $Fe_{83}Ga_{17}$ ribbons before and after heat treatment. (a) As-spun, (b) 650 °C, (c) 700 °C, (d) 750 °C.

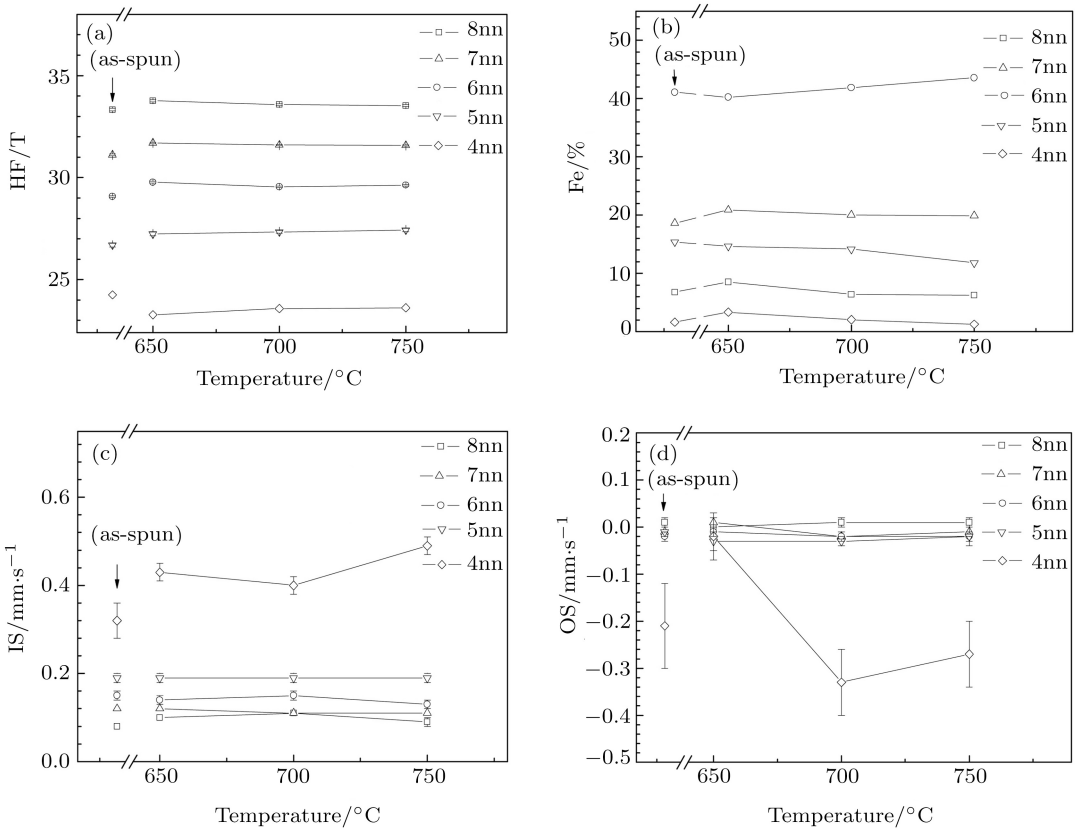


Fig. 5. Mössbauer parameters for $Fe_{83}Ga_{17}$ melt-spun ribbon: (a) HF, (b) IS, (c) QS, (d) the relative content Fe of each sub-spectrum.

4. Discussion

More attention should be paid to the 4nn sub-spectrum, since the main difference in structure between B2-like and DO_3 is the occupancy way and symmetry of the four Ga atoms. The QS value can reflect the non-spherical symmetry charge distribution at the Mössbauer nucleus and it indirectly reflects the occupancy of the Ga atoms neighbouring Fe atom. Thus, according to QS value, we are able to determine whether the 4nn sub-spectrum is the result of DO_3 phase or B2-like phase. Taking account of the arrangement of all atoms neighbouring the central Fe atoms, we can find that there is no Ga–Ga pair in the DO_3 structure but two Ga–Ga pairs in the B2-like structure as displayed in Fig. 6. Therefore, in order to verify the existence of Ga–Ga pair, other kinds of short range orders in DO_3 and A2 phases should be ascertained first.

In order to simplify the calculation, we assume that both DO_3 and B2-like phases have the same lattice constants. In a simple model, we consider the EFG of Fe nucleus with $y = 4$.

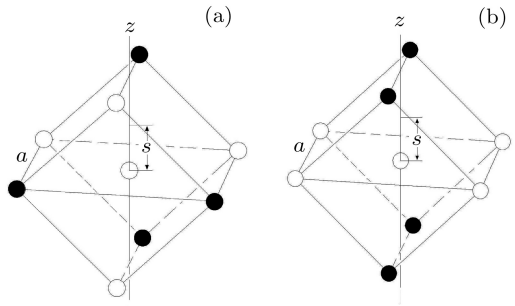


Fig. 6. Near neighbour arrangements for DO_3 and B2-like structures. (a) DO_3 structure, (b) B2-like structure (• Fe ◯ Ga).

If the neighbouring atoms in DO_3 structure are considered as point charges, the electric potential at the distance s, generated by the neighbour Fe and Ga atoms, can be expressed as

$$V_s^{\mathrm{Ga}} = \frac{2q_{\mathrm{Ga}}}{\left[\left(\frac{\sqrt{3}}{2}a\right)^2 + s^2\right]^{1/2}} + \frac{q_{\mathrm{Ga}}}{\left[\left(\frac{\sqrt{2}}{2}a - s\right)^2 + \left(\frac{a}{2}\right)^2\right]^{1/2}} + \frac{q_{\mathrm{Ga}}}{\left[\left(\frac{\sqrt{2}}{2}a + s\right)^2 + \left(\frac{a}{2}\right)^2\right]^{1/2}}, \tag{1}$$

$$V_s^{\mathrm{Fe}} = \frac{2q_{\mathrm{Fe}}}{\left[\left(\frac{\sqrt{3}}{2}a\right)^2 + s^2\right]^{1/2}} + \frac{q_{\mathrm{Fe}}}{\left[\left(\frac{\sqrt{2}}{2}a - s\right)^2 + \left(\frac{a}{2}\right)^2\right]^{1/2}} + \frac{q_{\mathrm{Fe}}}{\left[\left(\frac{\sqrt{2}}{2}a + s\right)^2 + \left(\frac{a}{2}\right)^2\right]^{1/2}}. \tag{2}$$

The EFG value at Fe-core is defined as the negative value of second derivative of electric potential. So the EFG of Ga atoms along the z-axis is obtained as

$$\frac{\mathrm{d}^2V_s^{\mathrm{Ga}}}{\mathrm{d}s^2} = q_{\mathrm{Ga}}\left\{\begin{array}{l} 3\left[\frac{a^2}{4} + \left(\frac{\sqrt{2}}{2}a - s\right)^2\right]^{-5/2}\left(\frac{\sqrt{2}}{2}a - s\right)^2 + 3\left[\frac{a^2}{4} + \left(\frac{\sqrt{2}}{2}a + s\right)^2\right]^{-5/2}\left(\frac{\sqrt{2}}{2}a + s\right)^2 \\ -\left[\frac{a^2}{4} + \left(\frac{\sqrt{2}}{2}a - s\right)^2\right]^{-3/2} - \left[\frac{a^2}{4} + \left(\frac{\sqrt{2}}{2}a + s\right)^2\right]^{-3/2} + 6s^2\left(\frac{3}{4}a^2 + s^2\right)^{-5/2} \\ -2\left(\frac{3}{4}a^2 + s^2\right)^{-3/2} \end{array}\right\}. \tag{3}$$

When $s \to 0$,

$$\frac{\mathrm{d}^2V_s^{\mathrm{Ga}}}{\mathrm{d}s^2} = 0.$$

Similarly, when $s \to 0$,

$$\frac{\mathrm{d}^2V_s^{\mathrm{Fe}}}{\mathrm{d}s^2} = 0.$$

Thus

$$V_{ss} = \frac{\mathrm{d}^2V^{\mathrm{Ga}}}{\mathrm{d}s^2} + \frac{\mathrm{d}^2V^{\mathrm{Fe}}}{\mathrm{d}s^2} = 0. \tag{4}$$

According to the above equations, the electric field gradient of DO_3 phase is zero along the z direction and so is the electric field gradient near the Fe-core in the plane perpendicular to the z axis.

Therefore, the electric field gradient of each neighbouring atoms of DO_3 is zero at the Fe nucleus centre. As a result, electric quadrupole splitting does not take place and the quadrupole splitting value is zero. Since this calculation is based on assumptions, the quadrupole splitting may not be zero exactly, but a near-zero value.

In the B2-like structure, the electric potentials of Ga and Fe atoms in the distance s are as follows:

$$V_s^{\mathrm{Ga}} = \frac{2q_{\mathrm{Ga}}}{\left[\left(\frac{a}{2}\right)^2 + \left(\frac{\sqrt{2}}{2}a - s\right)^2\right]^{1/2}} + \frac{2q_{\mathrm{Ga}}}{\left[\left(\frac{a}{2}a\right)^2 + \left(\frac{\sqrt{2}}{2} + s\right)^2\right]^{1/2}}, \quad (5)$$

$$V_s^{\mathrm{Fe}} = \frac{4q_{\mathrm{Fe}}}{\left[\left(\frac{\sqrt{3}}{2}a\right)^2 + s^2\right]^{1/2}}. \quad (6)$$

When $s \to 0$, the EFG values of Fe and Ga atoms along z-axis are

$$\frac{\mathrm{d}^2 V_s^{\mathrm{Ga}}}{\mathrm{d}s^2} = \frac{32q_{\mathrm{Ga}}}{3\sqrt{3}a^3}, \quad (7)$$

$$\frac{\mathrm{d}^2 V_s^{\mathrm{Fe}}}{\mathrm{d}s^2} = -\frac{32q_{\mathrm{Fe}}}{3\sqrt{3}a^3}. \quad (8)$$

For the B2-like phase, the EFG of each neighbour atom at Fe nucleus centre on each axis can be written as

$$V_{xx} = -\frac{8}{3\sqrt{3}a^3}(q_{\mathrm{Ga}} + q_{\mathrm{Fe}}), \quad (9)$$

$$V_{yy} = \frac{8}{3\sqrt{3}a^3}(q_{\mathrm{Ga}} + q_{\mathrm{Fe}}), \quad (10)$$

$$V_{zz} = \frac{32}{3\sqrt{3}a^3}(q_{\mathrm{Ga}} - q_{\mathrm{Fe}}). \quad (11)$$

As a result, the EFGs at three axes are not zero and EFG around the Fe-core is not zero either.

The different expressions of EFG along different axes suggest that the EFG is non-spherically symmetric. So we introduce a non-spherical symmetry factor η, which is 0.70 through calculation. The negative value of EFG along the z-axis leads the quadrupolar at the central Fe nucleus splitting to a value less than zero in the B2-like phase.

In summary, the Ga atoms and Fe atoms are spherically symmetrically distributed around the central Fe nucleus in DO_3 structure. For this reason, the electric field at Fe nucleus is spherically symmetric and the gradient is zero. However, for the B2-like structure, the neighbouring Ga atoms are distributed along the (110) plane. Consequently, the EFG generated by neighbouring Fe and Ga atoms could not balance out each other. Equally, it is non-spherically symmetric. So the value of QS is less than zero.

Now we come to Fig. 5(d). The QS values of 4nn sub-spectrum of the as-spun ribbon and the ribbons heat treated at 700 and 750°C are −0.21, −0.33 and −0.29 mm/s respectively. So we can conclude that the ribbons contain B2-like phase and the fact that Ga–Ga pairs exist in Fe–Ga alloy is confirmed. However, this does not rule out the possibility of DO_3 phase. Namely, the sub-spectrum may be a mixture of spectra of DO_3 and B2-like.

However, the B2-like structure does not always exist in the ribbons. Figure 5(d) shows that the QS value of 4nn sub-spectrum is around zero in ribbon heat-treated at 650°C. A potential explanation is that the main phase of these ribbons is DO_3 phase and the B2-like phase is not enough to be detected in the sense of the phase quantity.

5. Conclusion

The magnetostrictive properties of melt-spun $Fe_{83}Ga_{17}$ ribbons are improved after heat treatment. The maximum magnetostriction of −578.4 ppm is obtained in ribbon heat-treated at 750°C. Mössbauer analysis and theoretical calculation results reveal that the B2-like phase is obtained as expected. In conclusion, the B2-like structure is verified to be a useful short-range order phase for the improvement of magnetostrictive properties in Fe–Ga alloy.

Acknowledgment

The authors are grateful to Prof. Liu Milan from Jilin University for her help.

References

[1] Guruswamy S, Srisukhumbowornchai N, Clark A E, Restorff J B and Wun-Fogle M 2000 *Scripta Mater.* **43** 239

[2] Cheng S F, Das B N, Wun-Fogle M, Lubitz P and Clark A E 2002 *IEEE Tran. Mag.* **38** 2838

[3] Liu G D, Liu L B, Liu Z H, Zhang M, Chen J L, Li J Q, Wu G H, Li Y X, Qu J P and Chin T S 2004 *Appl. Phys. Lett.* **84** 2124

[4] Wu R Q 2002 *J. Appl. Phys.* **91** 7358

[5] Zheng L, Jiang C B, Shang J X and Xu H B 2009 *Chin. Phys.* B **18** 1647

[6] Zhang M C, Gao X X, Jiang H L, Qiao Y and Zhou S Z 2007 *J. Alloys Compd.* **431** 42

[7] Liu L B, Fu S Y, Liu G D, Wu G H, Sun X D and Li J Q 2005 *Phys.* B **365** 102

[8] Newkirk L R and Tsuei C C 1971 *J. Appl. Phys.* **42** 5250
[9] Perduta K, Olszewski J, Busbridge S and Nabialek M 2008 *Acta Phys. Pol.* A **114** 1537
[10] Gaudet J M, Hatchard T D, Farrell S P and Dunlap R A 2008 *J. Magn. Magn. Mater.* **320** 821
[11] Borrego J M, Blázquez J S, Conde C F, Conde A and Roth S 2007 *Intermetallics* **15** 193
[12] Basumatary H, Palit M, Arout Chelvane J, Pandian S, Manivel Raja M and Chandrasekaran V 2008 *Scripta Mater.* **59** 878
[13] Dunlap R A, Deschamps N C, Mar R E and Farrell S P 2006 *J. Phys.*: *Condens. Matter* **18** 4907
[14] Dunlap R A, Gaudet J M and Hatchard T D 2008 *J. Magn. Magn. Mater.* **320** 2730
[15] Zhao X, Mellors N, Kilcoyne S, Lord D, Lupu N, Chiriac H and Henry P F 2008 *J. Appl. Phys.* **103** 07B320
[16] Lograsso T A and Summers E M 2006 *Mater. Sci. Eng.* A **416** 240
[17] Dunlap R A, McGraw J D and Farrell S P 2006 *J. Magn. Magn. Mater.* **305** 315